Journal of Glaciology

Article

Cite this article: Zhai Z, Wang Y, Reijmer CH, Smeets PCJP, Zhang X, Zhang W (2024). MODIS land surface temperature in East Antarctica: accuracy and its main affecting factors. *Journal of Glaciology* **70**, e22, 1–12. https://doi.org/10.1017/jog.2024.17

Received: 12 January 2023
Revised: 28 January 2024
Accepted: 30 January 2024

Keywords:
accuracy; East Antarctic Ice Sheet; ice surface temperature; influencing factors; MODIS

Corresponding author:
Yetang Wang;
Email: yetangwang@sdnu.edu.cn

cambridge.org/jog

MODIS land surface temperature in East Antarctica: accuracy and its main affecting factors

Zhaosheng Zhai[1], Yetang Wang[1], Carleen H. Reijmer[2], Paul C. J. P. Smeets[2], Xueying Zhang[1] and Wuying Zhang[1]

[1]College of Geography and Environment, Shandong Normal University, Jinan 250014, China and [2]Institute for Marine and Atmospheric Research Utrecht, Utrecht University, Utrecht, The Netherland

Abstract

Recently released Moderate-Resolution Imaging Spectroradiometer (MODIS) land surface temperature (LST) collection 6.1 (C6.1) products are useful for understanding ice–atmosphere interactions over East Antarctica, but their accuracy should be known prior to application. This study assessed Level 2 and Level 3 MODIS C6.1 LST products (MxD11_L2 and MxD11C1) in comparison with the radiance-derived in situ LSTs from 12 weather stations. Significant cloud-related issues were identified in both LST products. By utilizing a stricter filter based on automatic weather station cloud data, despite losing 29.4% of the data, accuracy of MODIS LST was greatly improved. The cloud-screened MODIS LST exhibited cold biases (−5.18 to −0.07°C, and root mean square errors from 2.37 to 6.28°C) than in situ LSTs at most stations, with smaller cold biases at inland stations, but larger ones at coastal regions and the edge of plateau. The accuracy was notably higher during warm periods (October–March) than during cold periods (April–September). The cloud-screened MODIS C6.1 LST did not show significant improvements over C5 (Collection 5) version across East Antarctica. Ice-crystal precipitation occurring during temperature inversions at the surface (T_{air}-$T_{surface}$) played a crucial role in MODIS LST accuracy on inland plateau. In coastal regions, larger MODIS LST biases were observed when the original measurements were lower.

1. Introduction

The East Antarctic Ice Sheet (EAIS) is always a region of interest due to its critical role in the climate system of the Earth (Studinger and others, 2005; Seo and others, 2016) and its possession of the largest ice volume, equivalent to ~52 m of global sea level (Pattyn and Morlighem, 2020). In recent decades, the EAIS was considered to be less susceptible to climate warming (Remy and Frezzotti, 2006) than the Arctic (Graversen and others, 2008), West Antarctica (Steig and others, 2009) and Antarctic Peninsula (Vaughan and others, 2003). However, mass loss has recently been observed in the EAIS coastal regions, including Wilkes Land and Northern Victoria Land (Rignot and others, 2008; Miles and others, 2013; Mengel and others, 2014), thereby causing the global sea level rise. The regional mass loss in these regions was associated with Circumpolar Deep Water modified by warming (Miles and others, 2013), suggesting that the Earth's largest ice sheet was likely more sensitive to climate change than previously recognized. Various climate projections indicated that the Antarctic Ice sheet melting could contribute ~1 m to global sea level rise by 2100 (DeConto and Pollard, 2016). However, the extent of the EAIS's contribution to future sea level rise under future climate warming remained highly uncertain (Wong and others, 2017). In this context, it is imperative to make accurate and extensive temperature measurements, and subsequently to re-evaluate the sensitivity of the EAIS to temperature changes.

The land surface temperature (LST) reflects the energy budget at the land surface, and its long-term variations across the EAIS have the potential to significantly alter the surface mass balance and thus affect the ice-sheet stability (Remy and Frezzotti, 2006; Tuckett and others, 2019; Baumhoer and others, 2021). It also impacts changes in atmospheric circulation (Bromwich and Wang, 2008; Clem and Fogt, 2015; Screen and others, 2018) and polar terrestrial ecosystems (Amesbury and others, 2017). Although considerable efforts have been made to establish staffed weather stations for meteorological observations on the Antarctic continent since the International Geophysical Year (IGY) of 1957/1958, among them only three (Dome C, South Pole and Syowa Stations also included in the Baseline Surface Radiation Network [BSRN]) can provide continuous longwave radiation measurements for the estimation of surface skin temperature (Driemel and others, 2018). Since the 1980s, more than 260 automatic weather stations (AWSs) have been set up in Antarctica (Allison and others, 1993; Turner and others, 2004; Lazzara and others, 2012; Wang and others, 2023), some of which alternatively offer skin temperature measurements. However, until recently, in situ surface temperature observations have been extremely sparse in space and time largely because of the harsh environmental conditions.

Benefiting from the short revisiting cycle and extensive spatial coverage, satellites have enabled faster retrieval of skin temperature across the entire EAIS (Comiso, 2000; Retamales

and others, 2019). Numerous spaceborne sensors including Advanced Spaceborne Thermal Emission and Reflection Radiometer (ASTER) (Wang and Liang, 2009; Duan and others, 2017), Thematic Mapper (TM) (Nguemhe Fils and others, 2018), Enhanced Thematic Mapper Plus (ETM +) (Kumari and others, 2018), Moderate-Resolution Imaging Spectroradiometer (MODIS) (Wan and others, 2002, 2004) and Thermal Infrared Sensor (TIRS) (Tan and others, 2017), are currently used to generate thermal infrared (IR) LST products. Although ASTER (90 m) and Landsat (TM/ETM + /TIRS, 30 m) products have higher spatial resolution than MODIS, their longer revisit cycle (~16 d) constrains their application in detecting daily LST variations. Owing to high temporal resolution, MODIS-derived LST products, covering the period from 2000 onwards, have been widely applied in many fields (e.g. Xu and Shen, 2013; Kilpatrick and others, 2015; Qie and others, 2020), especially in inaccessible polar regions, such as reconstruction of near-surface air temperature (Zhang and others, 2022), investigation of LST patterns (Kang and others, 2014; Retamales and others, 2019) and determination of surface melting of the ice sheets (Nghiem and others, 2012; Hall and others, 2013).

Various validations or comparisons of the MODIS LST C5 and C6 products have already been conducted in non-polar regions, such as the Savannah landscape (Jacob and others, 2004), city (Ayanlade, 2016), cropland (Coll and others, 2005, 2009), inland water (Wan and others, 2008; Crosman and Horel, 2009), permafrost (Muster and others, 2015), bare soil surfaces (Duan and others, 2017), sand dune and forest (Li and others, 2014; Duan and others, 2018). The offsets of MODIS LST values from in situ measurements were generally within 1°C for most surface types (Wan and others, 2004; Wan, 2014). For the cryosphere, the validations of MODIS LST have been performed in the Arctic (Hall and others, 2008; Koenig and Hall, 2010; Westermann and others, 2012; Østby and others, 2014) and alpine mountains (Williamson and others, 2017; Kindstedt and others, 2022). However, studies concerning this topic were relatively rare in Antarctica (Wang and others, 2013; Liu and others, 2015), likely due to the limited availability of in situ skin temperature observations. Most recently, a preliminary assessment of accuracy of MODIS LST C5 products was conducted in East Antarctica (Freville and others, 2014). Scambos and others (2018) also compared MODIS C5 and C6 LST with air temperature data from weather stations during winter in the upper East Antarctic ice divide. Nevertheless, the latest version (C6.1) of the MODIS LST product remains unvalidated in East Antarctica, and the factors influencing its accuracy should be explored.

The main objective of this study was to assess the accuracy of the recently released MODIS C6.1 LST swath product across East Antarctica, using the in situ LSTs calculated by longwave radiation measurements at 12 weather stations. The factors affecting MODIS LST accuracy were also examined to identify potential enhancements for the ongoing algorithm development.

2. Data and methods

2.1. MODIS LST products

The MODIS instruments onboard the Terra and Aqua spacecraft on the NASA Earth Observation System offer important observations of atmospheric water vapor, land surface conditions, cloud properties, aerosols and surface temperature, etc., over the entire Earth's surface every 1–2 d (Justice and others, 1998). This study utilized the LST products generated by a generalized split-window LST algorithm using the emissivity in band 31 (≈11 μm) and band 32 (≈12 μm) developed by Wan and Dozier (1996). The MODIS LST family has undergone several updates since the release of the first version. Here, we assessed the MOD/MYD11 collection 6.1 (C6.1) Level 2 swath products (here called MxD11_L2) from the Terra and Aqua satellites, which provided per-pixel LST values with a pixel size of 1 km and severed as the basis for the MODIS LST Level 3 products. On average, the available LSTs from the MxD11_L2 product were approximately five times per day at the coastal regions and more than nine times per day on the Antarctic Plateau. This most recent LST product made several calibration enhancements, including modification to the response-versus-scan angle (RVS) approach affecting reflectance bands for MODIS instruments, and adjustments of the optical crosstalk in IR bands of Terra MODIS (Wan and others, 2021). We also assessed the gridded MxD11C1 dataset, a Level 3 LST product at a spatial resolution of $0.05 \times 0.05°$ in an equal-angle geographic projection, which had four LST values at four distinct overpass times in a day (twice each at the Aqua and Terra satellites). Quality Control Science Dataset (QC SDS) were included in the two products. We selected only those LST values at each gridcell flagged as 'good quality' in the QC layer, which only contained the pixels under clear-sky conditions at a confidence level (defined in the MxD35 cloud mask product) of ≥95% above the land surface.

2.2. In situ measurements

The downwelling and upwelling longwave radiation (LW_{down} and LW_{up}) records at 12 stations (Fig. 1) were collected to determine snow skin temperatures, and subsequently to validate MODIS LST products. These stations comprised nine AWSs (Jakobs and others, 2020) and three BSRN stations (Driemel and others, 2018), each with records at varying timespans (Table 1). AWSs and BSRN stations provided hourly and minute-by-minute radiation records, respectively. Of these, two BSRN stations (DOM and SPO) and two AWSs (AWS12 and AWS13) were situated on the East Antarctic Plateau, whereas three AWS stations (AWS5, AWS10 and AWS11) and the SYO BSRN station were distributed along the coast of the EAIS. AWS6, AWS8, AWS9 and AWS16 were located at the edge of the plateau (Fig. 1). If LW_{up} is lower than LW_{down} of +5 W m^{-2}, the corresponding radiation values were excluded to ensure the accuracy of the observations (Freville and others, 2014). According to the Stefan–Boltzmann law, the snow skin temperature (T_s) was calculated by LW_{down} and LW_{up} at the stations via the following formula.

$$Ts = \sqrt[4]{\frac{LW_{up} - (1-\varepsilon)\, LW_{down}}{\varepsilon\sigma}} \quad (1)$$

where T_s represented the snow skin temperature (hereafter, in situ T_s), σ was the Stefan–Boltzmann constant (5.67×10^{-8} W m^{-2} K^{-4}) and ε denoted the snow surface emissivity. The surface emissivity of snow was estimated to be between 0.985 and 0.990 for all grain sizes (Dozier and Warren, 1982). Sensitivity tests by Freville and others (2014) showed that setting the snow surface emissivity to 1.0 and 0.98 in comparison to 0.99 resulted in an average surface temperature difference of only ~0.08°C (0.080 and 0.079°C, respectively). Thus, we used a constant snow surface emissivity value of 0.99 to calculate the in situ T_s (Brun and others, 2011).

At all 12 stations, we recorded in situ T_s within 5 min of the view time (hereafter, satellite overpass time) provided by the MODIS LST products. The mean bias (*MB*), root mean square error (*RMSE*) and determination coefficient (R^2) were used to quantify the uncertainties of the MODIS LST products.

$$\text{Mean bias} = \frac{\sum_{i=1}^{n} (y_i - t_i)}{n} \quad (2)$$

https://doi.org/10.1017/jog.2024.17 Published online by Cambridge University Press

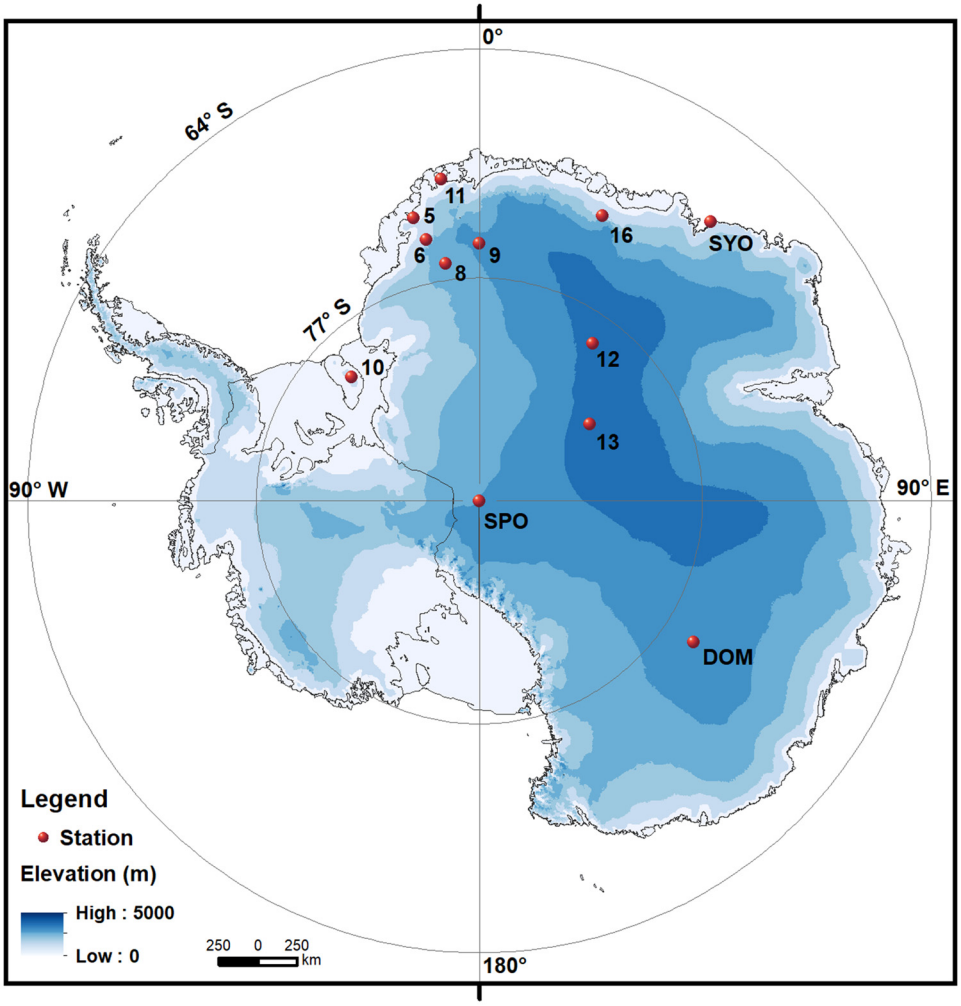

Figure 1. Map of the study area and the weather station locations.

$$RMSE = \sqrt{\frac{\sum_{i=1}^{n}(y_i - t_i)^2}{n}} \quad (3)$$

$$R^2 = 1 - \frac{\sum_{i=1}^{n}(y_i - t_i)^2}{\sum_{i=1}^{n}(t_i - \bar{t})^2} \quad (4)$$

$$r_{yt} = \frac{\sum_{i=1}^{n}(t_i - \bar{t})(y_i - \bar{y})}{\sqrt{\sum_{i=1}^{n}(t_i - \bar{t})^2}\sqrt{(y_i - \bar{y})^2}} \quad (5)$$

where n, y_i and t_i were the number of in situ observations, the MODIS LST values and in situ T_s, respectively. $\bar{y}$ and $\bar{t}$ were the average of satellite-derived and in situ surface temperatures, respectively.

To more effectively remove cloud contamination from MODIS LST pixels, and to identify the environmental factors affecting the accuracy of satellite-derived LSTs, the cloud fraction, 2 m air temperature (T_{2m}), solar radiation, wind speed and relative humidity observations from the nine AWSs were used. The cloud fraction is the physically meaningful cloud cover obtained from the longwave radiation balance measured by the AWS and was calculated based on the difference in emissivity between clear and cloudy atmospheres. Kuipers Munneke and others (2011) plotted the hourly LW_{down} against the T_{2m} data in a scatterplot. The upper boundary of the scatterplot coincided with $LW_{down} = \sigma T_{2m}^4$ (atmospheric emissivity $\varepsilon \approx 1$, completely cloudy-sky emitting as a blackbody radiator); the lower boundary of the scatterplot could be approximately fitted by a second-order polynomial to represent clear-sky conditions ($\varepsilon \approx 0$). The cloud fraction (between 0 and 1) was produced using linear interpolation between the two boundaries (details in Kuipers Munneke and others, 2011). Using these cloud fraction data, we set up a filter to eliminate cloud-contaminated MODIS LSTs. MODIS LST grid cells with the corresponding AWS cloud fraction exceeding the threshold of 0.3 were classified as cloud-contaminated, and subsequently screened out. After removing the cloud-contaminated values, Pearson's correlation coefficient (r_{yt}) was employed to quantify the relationships between meteorological factors and the biases in the two sets of skin temperature data.

3. Results

3.1. Accuracy of the MODIS LST products

3.1.1. Accuracy of the original MxD11_L2 and MxD11C1 LST products at satellite overpass times

At all the stations, the biases between the MxD11_L2 LST and in situ T_s predominantly fell below 0°C (Figs 2, 3), with the highest frequency between −4 and 0°C, suggesting that the MODIS LST was generally lower than in situ T_s in most of the cases. Specially, the MODIS LST exhibited mean cold biases ranging from −4.86 to −0.66°C relative to the near-synchronous in situ

https://doi.org/10.1017/jog.2024.17 Published online by Cambridge University Press

Table 1. Summary of the station information

Station	Latitude °S	Longitude	Elevation m	Data time spans
Syowa (SYO)	69.01	39.59°E	18	January 2010–December 2014
AWS5	73.10	13.17°W	360	January 2010–February 2014
AWS11	71.17	6.80°W	690	January 2010–December 2014
AWS10	79.57	45.78°W	890	February 2003–July 2005
AWS6	74.47	11.52°W	1160	January 2004–December 2008
AWS16	71.95	23.33°E	1300	January 2010–December 2014
AWS8	76.00	8.05°W	2400	January 2002–January 2003
AWS9	75.00	0°	2900	January 2010–December 2014
Dome C (DOM)	75.10	123.38°E	3233	January 2013–December 2013
AWS12	78.65	35.63°E	3620	January 2008–March 2010
AWS13	82.17	55.03°E	3730	January 2010–December 2014
South Pole (SPO)	89.98	24.80°W	2800	January 2013–December 2013

All stations were divided into three groups by their elevations. The first four stations (AWS5, AWS10, AWS11 and SYO) were classified as the coastal group (<1000 m) and the last four (AWS12, AWS13, DOM and SPO) as the plateau group (>3000 m). The middle four (AWS6, AWS9, AWS8 and AWS16) were classified as the group located on the edge of the plateau (1000–3000 m)

T_s, with the exception of a minor warm bias (0.11°C) at the Syowa station. The *RMSE* values ranged from 3.7 to 7.32°C, and R^2 values exceeded 0.75 at the majority of stations. Spatially, cold biases were less pronounced at stations on the East Antarctic Plateau (−1.39 to −0.66°C) and more significant at those along the edge of plateau (−4.86 to −1.68°C), with coastal stations showing intermediate values (−3 to −1.76°C). In contrast, the R^2 values were relatively low for the stations at the edge of plateau (0.59–0.84), higher for those on plateau (0.76–0.91) and for coastal stations (0.64–0.83) still in between. However, these spatial patterns were not observed in the *RMSE*s.

Similarly, compared with the in situ T_s, the MxD11C1 LST exhibited mean cold biases (−5.27 to −0.48°C), except for a slight warm bias (0.17°C) at the Syowa station, with *RMSE* values ranging from 3.17 to 6.46°C and R^2 exceeding 0.7 at all stations (Fig. S1). The spatial pattern of the MxD11C1 LST biases was also the same as that of the L2 product, indicating smaller biases at stations on the East Antarctic Plateau (−1.07 to −0.48°C) and larger ones along the edge of plateau (−5.27 to −4.49°C), with the intermediate values at coastal stations (−1.84 to 0.17°C). The R^2 values were relatively low for the stations at the edge of plateau (0.7–0.73), higher for those on the plateau (0.87–0.94) and intermediate for coastal stations (0.76–0.89). These results basically coincided with those of the MxD11_L2 product in terms of magnitude.

A large numerous of sample points were observed well below the 1:1 line at almost all stations (Fig. 3), suggesting substantial cold biases in MODIS LST in comparison to in situ T_s. In particular, some bias values dipped below −20°C (Fig. 2). Spatially, these large cold biases were more prevalent at stations near the coast, while they were comparatively infrequent on the Antarctic Plateau. A possible reason for these large biases was the imperfect cloud mask of MODIS LST products, as noted in earlier studies on previous MODIS LST versions in Greenland (Hall and others, 2004; Westermann and others, 2012; Adolph and others, 2018). Since the temperature of clouds tend to be much lower than that of snow surface, misidentification of cloud and snow surfaces can limit the accuracy of surface temperature products in ice- and snow-covered regions. This could be further confirmed by the significant correlations between the MODIS LST biases and AWS cloud fraction (Table 2). Seasonally, this phenomenon occurred more frequently during warm periods than during cold periods (Fig. 3 and Table 2). Therefore, we initially implemented a more restrictive cloud mask based on AWS cloud fraction to further reduce the effects of cloud on the MODIS LST. Due to the absence of cloud records at the three BSRN stations, it was not possible to reduce cloud contamination using a unified filter, and thus these data were not included in the following analyses.

3.1.2. Accuracy of the MxD11_L2 LST through filtering by in situ cloud data

As shown in Figure 4, the stricter cloud mask based on the AWS cloud fraction greatly reduced the number of cloud-affected LST measurements, and the filtered MODIS LST could be considered to be cloud-free. Even after filtering out the cloud effects by means of AWS cloud data, the MODIS LST still exhibited cold biases (−5.18 to −0.33°C) in comparison to in situ T_s at all AWSs (Fig. 4). The *RMSE* values varied between 2.37 and 6.28°C, and R^2 values ranged from 0.72 to 0.95. Clearly, by reducing the impacts of cloud, accuracy of the MODIS LST was notably improved at all stations except AWS9. Specially, the MODIS LST biases decreased by ~1°C at these stations. The *RMSE* values reduced by 0.16–2.26°C, with an average of 1.39°C, and R^2 rose by 0.04–0.18 with an average of 0.09. Spatially, the improvement in MODIS LST accuracy was most pronounced at the stations located along the Antarctic coast and the edge of plateau. The *RMSE*s reduced by more than 1°C and R^2 values increased by more than 0.1 at almost all stations. This indicated that cloud cover significantly impacted the MODIS LST accuracy in these regions. However, at AWS9, the improvement in LST accuracy was minimal, with a slight increase in *RMSE* and bias by 0.09 and 0.32°C, respectively. This can be explained by no significant correlation between MODIS LST biases and cloud fraction (Table 2), suggesting that factors other than cloud conditions primarily affect the MODIS LST accuracy here.

We calculated the daily averages of MODIS LST and in situ T_s respectively to examine the performance of the satellite-derived LST on daily scale. Relative to the corresponding in situ T_s (Fig. 5), the daily-averaged MODIS LST still presented cold biases at all stations (−5 to −0.39°C). The *RMSE* values ranged from 1.47 to 5.65°C, which were lower than those at satellite overpass times in magnitude. The R^2 at these stations also increased, with all above 0.73 and most above 0.9. Spatially, MODIS LST accuracy improvement was most prominent at stations on the Antarctic coast and on the plateau, with the R^2 values of above 0.87, the *RMSE* values of below 3.1°C and cold biases of smaller than −1.52°C. For the stations located at the edge of the plateau, the LST accuracy was relatively higher in AWS6 and AWS8, while there was still more room for improvement in AWS9 and AWS16.

3.1.3. Cloud-screened MODIS LST accuracy for the monthly periods

Aggregating the data into daily periods led to closer agreement between the MODIS LST and in situ T_s (see the description above and Figs 4, 5). To determine if the monthly synthesis can result in more robust alignment, the mean monthly biases of the two datasets were calculated. As shown in Figure 6, the

https://doi.org/10.1017/jog.2024.17 Published online by Cambridge University Press

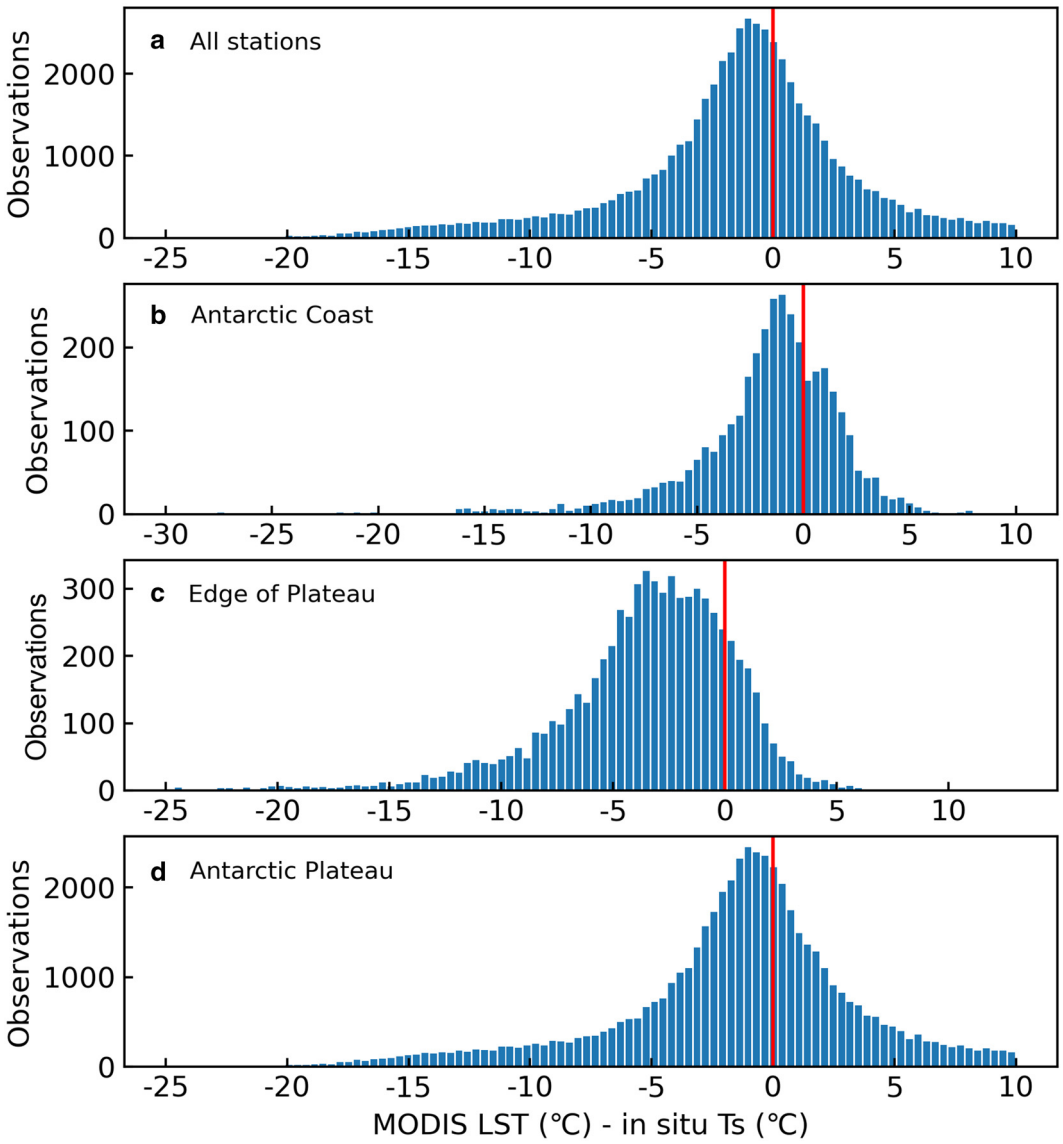

Figure 2. Histograms of the biases between the MODIS LST and in situ T_s at (a) all stations, (b) Antarctic coast, (c) edge of the plateau and (d) Antarctic Plateau. The red vertical line denoted the bias value equal to 0.

difference between the two datasets was not eliminated by the monthly synthesis. We found that the biases showed a distinct seasonality at stations along the coast and the edge of plateau, with larger biases during the cold period (April to September), peaking during May–July, and smaller biases during the warm period (October to March). Both the means and medians of biases were below 0°C for each month with the mean values obviously lower than the medians. This pattern was also evident across all stations (Fig. 6a). Unfortunately, the relatively low pair counts (no more than 25) between the two datasets limited their statistical significance during the cold period at plateau stations, leading to the omission of the results for those months (Fig. 6d). During the warm period, the monthly biases were maintained at a low level at these stations, indicating the high accuracy of the MODIS LST.

3.2. Factors influencing the MODIS LST accuracy in East Antarctica

Cloud fraction, near-surface temperature inversion intensity (T_{air}–$T_{surface}$) and original MODIS LST were potential causes of the discrepancies between the MODIS LST and in situ T_s. As previously mentioned, cloud contaminations significantly affect the MxD11_L2 LST accuracy over EAIS. Given that the MxD11_L2 LST served as the input for the generation of MxD11C1, and that no additional cloud-reducing algorithms were applied, cloud issues still occurred in MxD11C1. This was further confirmed by the similar accuracies of MxD11_L2 LST and MxD11C1. Near-surface inversions are widespread on the EAIS (Hudson and Brandt, 2005; Scambos and others, 2006, 2018; Pietroni and others, 2014) and typically occur under clear-sky conditions, low incoming solar irradiance and low wind speeds (Table S2 and Fig. S2). In this study, the difference between T_{air} and $T_{surface}$ was calculated to estimate the near-surface inversion intensity. The value (T_{air}–$T_{surface}$) is positive when the 2 m air temperature is higher than the snow surface temperature, indicating the occurrence of near-surface temperature inversion. Cloud-screened MODIS LST biases correlated significantly with near-surface temperature inversions at all stations (−0.34 to 0.69, $p < 0.05$) during satellite overpass times (Fig. 7a). By comparison, the correlations at plateau stations were higher than those at the coastal stations, peaking in summer or fall (0.6–0.88, $p < 0.05$). Conversely, correlations at coastal stations did not exhibit clear seasonality. For stations at the edge of plateau, the correlation pattern was similar to that of two plateau stations

https://doi.org/10.1017/jog.2024.17 Published online by Cambridge University Press

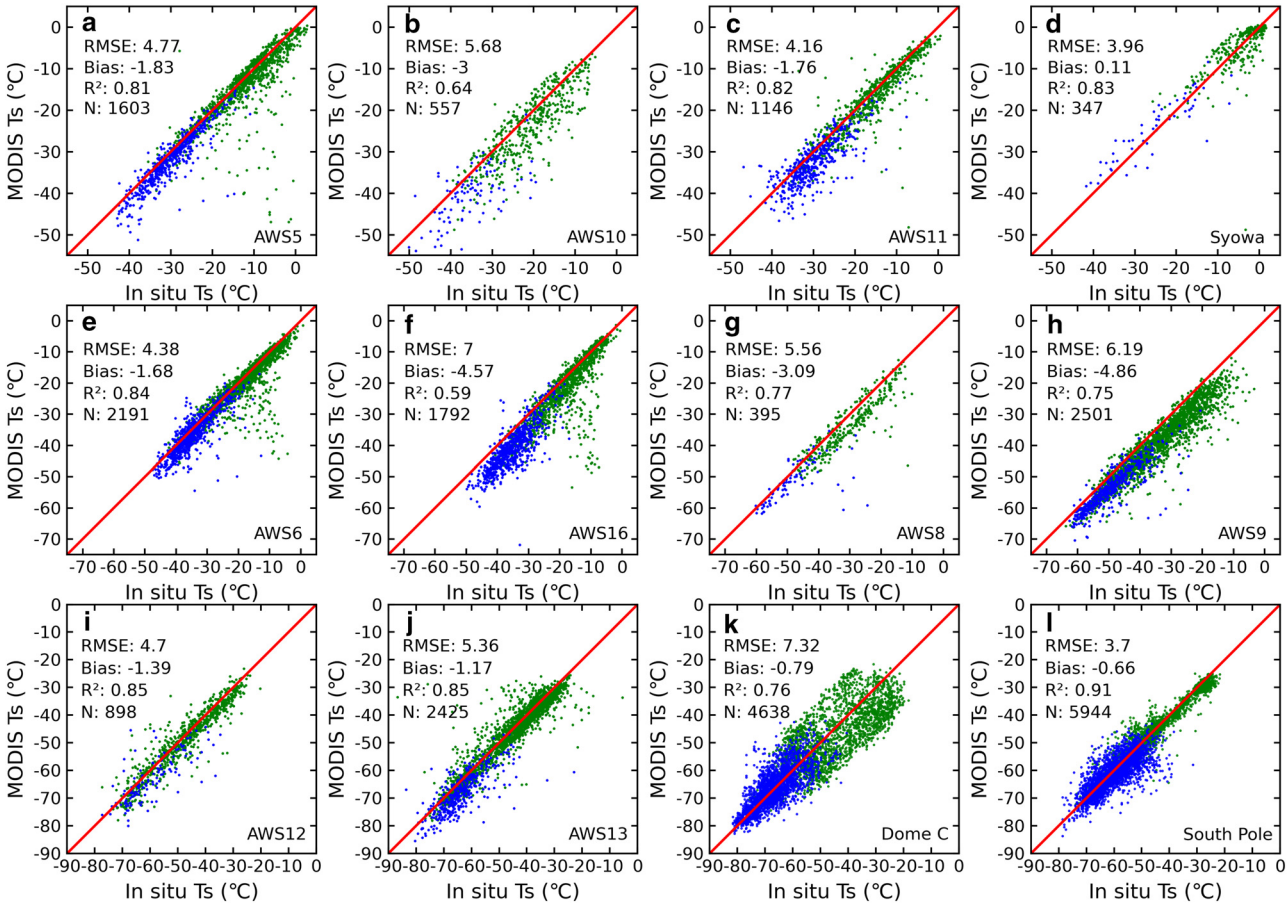

Figure 3. comparison between the MODIS LST and in situ T_s at satellite overpass times at stations located on the Antarctic coast (top group, a–d), the edge of the plateau (middle group, e–h) and the East Antarctic Plateau (bottom group, i–l). The red line represented the one-to-one line. The green and blue points represented the samples in warm period (October to March of the following year) and cold period (April to September), respectively. N stood for the paired amount of two types of LST observations.

(AWS8 and AWS9), possibly due to their higher elevations and greater distance from the ocean. In particular, the MODIS LST biases at AWS9 appeared to be associated with temperature inversions rather than cloud variations (Table 2). In contrast, AWS6 resembled coastal stations because of its lower elevation and closer proximity to the coast.

Significant correlations between biases and MODIS LST measurements were observed at the stations near the coast (AWS6, AWS16 and coastal stations; Fig. 7b). Seasonally, these correlations were highest in austral winter, a period characterized by more frequent occurrence of extreme low temperatures in MODIS LSTs. This difference was most pronounced at AWS16, where all correlation coefficients were above 0.52 ($p < 0.05$) at all scales. This means that when the original MODIS LST values were lower in the coastal region, their biases tended to be larger.

4. Discussion

To our knowledge, this study provided the first assessment of the accuracy of the latest MODIS C6.1 product over East Antarctica using available surface radiation-derived in situ T_s. Our results suggested that this MODIS LST product had a good performance in fitting in situ T_s, which was relatively accurate in aiding our understanding LST spatiotemporal patterns and ice–atmosphere interactions across the EAIS. However, cloud contamination emerged as a critical factor affecting MODIS LST accuracy, which was consistent with the findings from several previous studies on polar regions (Hall and others, 2008; Østby and others, 2014; Sun and others, 2017; Zhang and others, 2018). In this study, we chose to use clear-sky MODIS LST values flagged as 'good quality'. However, significant correlations (−0.56 to −0.39, $p < 0.05$) were observed between AWS cloud fraction and MODIS LST biases at all stations except AWS9, especially during the warm period characterized by higher cloud fraction (Fig. 3 and Table 2). Many cloud-contaminated data could also be found in the scatterplot (Fig. 3). This indicated that the current cloud mask algorithm of MODIS LST product was imperfect, and only partially effective over the EAIS. The pixels contaminated by clouds were not fully identified and excluded, which likely contributed much to the large cold biases (Fig. 3). Despite losing 29.4% of the data, the application of AWS cloud fraction as a stricter filter to remove cloud contamination resulted

Table 2. Correlation coefficients (r) between AWS cloud fraction and the biases of original MODIS LST at different AWSs

	AWS5	AWS6	AWS8	AWS9	AWS10	AWS11	AWS12	AWS13	AWS16
Whole period	**−0.51**	**−0.51**	**−0.31**	0.10	**−0.38**	**−0.38**	**−0.36**	**−0.41**	**−0.52**
Warm period	**−0.58**	**−0.60**	**−0.40**	0.12	**−0.38**	**−0.40**	**−0.31**	**−0.36**	**−0.64**
Cold period	**−0.31**	**−0.36**	**−0.18**	−0.05	**−0.32**	**−0.38**	**−0.32**	**−0.31**	**−0.26**

Bolded r values were statistically significant at $p < 0.05$ level.

https://doi.org/10.1017/jog.2024.17 Published online by Cambridge University Press

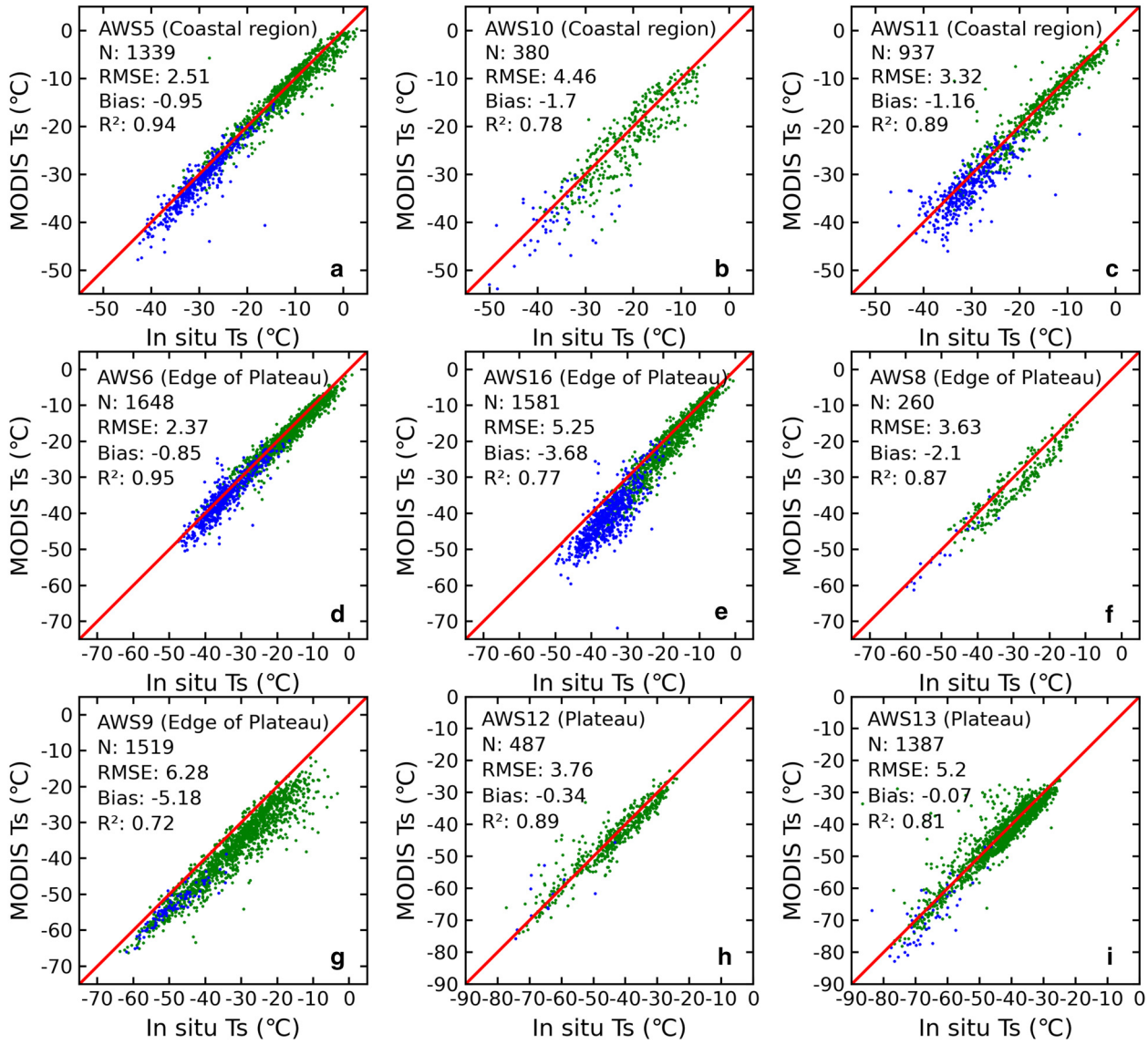

Figure 4. Comparison between in situ T_s and the MODIS LST after removing cloud-affected data at the satellite overpass times at stations located on the Antarctic coast (a–c), the edge of the plateau (d–g) and the East Antarctic Plateau (h–i). The red line represented the one-to-one line. The green and blue points represented the samples during warm period (October to March of the following year) and during cold period (April to September), respectively. N was the paired amount of two types of LST observations.

in the significant decreases in the biases and *RMSE*s between the two LST datasets, along with an increase in R^2. The improvement was more obvious at the stations located along the coast and the edge of plateau (Figs 3, 4), suggesting that cloud contamination occurred more frequently in places near the coast where air was relatively moist, and less on inland plateau where the sky was clearer. The MxD11_L2 LST was the original swath product of MODIS LST family and provided the input for the generation of Level 3 LST products. If a deficient cloud mask was employed, the accuracy of Level 3 product will likely be compromised. We verified this phenomenon using the MxD11C1 product at several stations with longer time series (Fig. S1). At these stations, the MxD11C1 LST exhibited cold biases (−5.27 to −0.48°C) with respective to the in situ T_s, except for a slight warm bias (0.17°C) at the Syowa station. The spatial pattern of the MxD11C1 LST biases was also the same as that of the L2 product. These bias values were basically coincided with the magnitude of the original MxD11_L2 product (without using AWS data to remove cloud effects), and the impact of cloud on the MODIS LST was largely retained in the Level 3 product (Fig. 3 and Fig. S1).

Cloud-screened MODIS LSTs still exhibited significant cold biases relative to in situ T_s at different timescales, which was in accordance with previous validations focusing on ice-covered polar regions (Scambos and others, 2006, 2018; Koenig and Hall, 2010; Westermann and others, 2012; Østby and others, 2014; Zikan and others, 2023). The bias and *RMSE* values were comparable in magnitude to those found in earlier estimation of the previous version of the MODIS LST at these sites. The MODIS Version C5 LST in East Antarctica showed cold biases (−2.66 to 0.08°C) in 2009, with worse accuracy at coastal stations (Freville and others, 2014). This seemed to show that there was no distinct improvement of C6 MODIS LST over C5 version across the EAIS. We further explicitly presented the spatial differences in biases, with the smaller cold biases occurring at the stations on the Antarctic plateau, but the larger biases occurring at those along the edge of plateau, and biases at coastal stations roughly in between. Accurate calibration of these deviations was essential to faithfully represent meteorological and glaciological conditions.

Near-surface temperature inversions also strongly influenced the MODIS LST accuracy. Previous studies showed that larger

https://doi.org/10.1017/jog.2024.17 Published online by Cambridge University Press

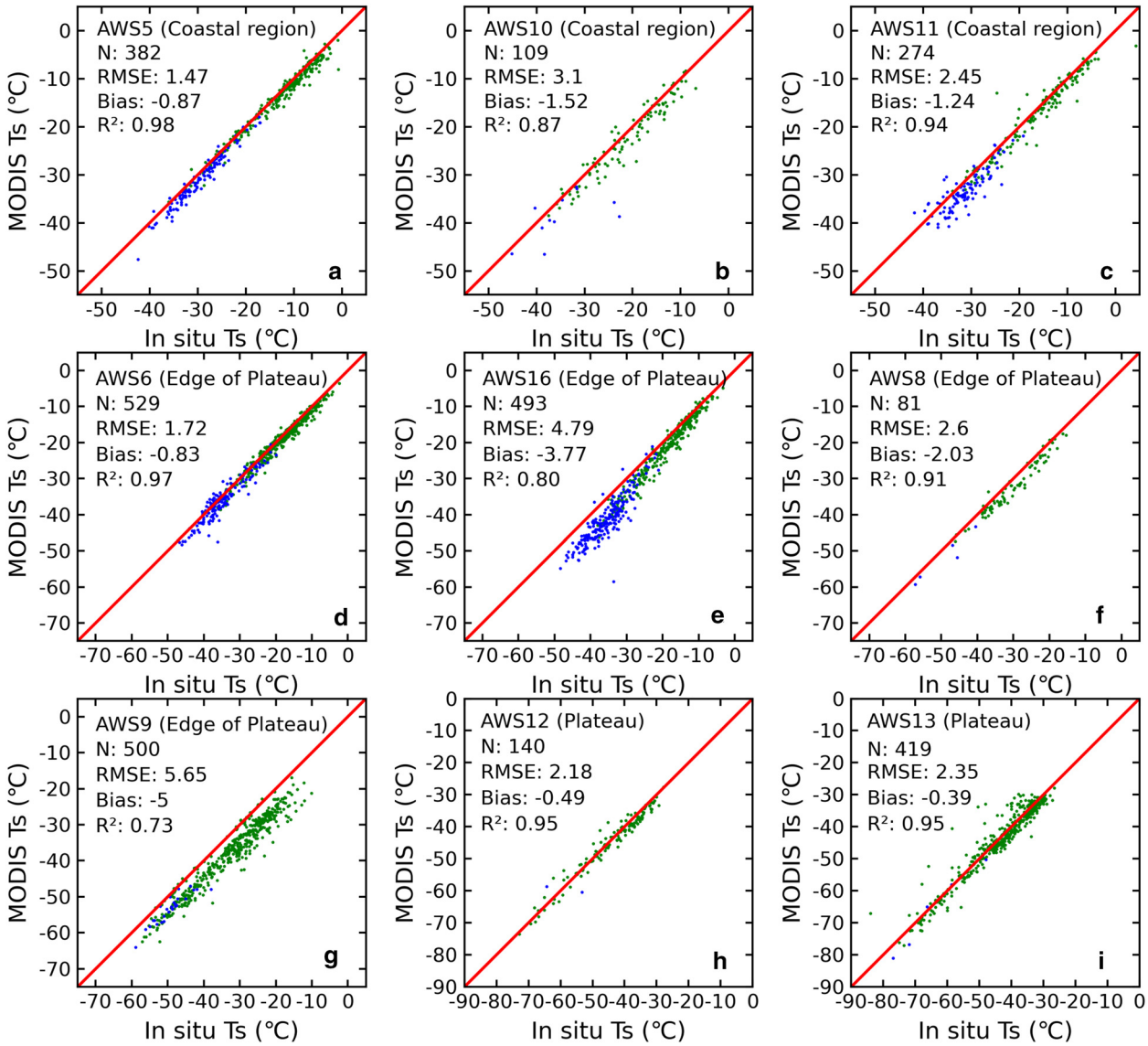

Figure 5. Comparison between in situ T_s and the MODIS LST after removing cloud-affected data at the daily-scale at the stations located on the Antarctic coast (a–c), the edge of the plateau (d–g) and the East Antarctic Plateau (h–i). The red line represented the one-to-one line. The green and blue points represented the samples during warm period (October to March of the following year) and during cold period (April to September), respectively. N was the paired amount of two types of LST observations.

cold biases of MODIS LST compared to 2 m air temperatures occur under stronger inversions in polar regions (Scambos and others, 2006, 2018; Adolph and others, 2018; Kindstedt and others, 2022). When comparing the MODIS LST with 2 m air temperatures in a test focusing on the EAIS, similar conclusions were drawn. When strong temperature inversions occurred, the in situ 2 m air temperature was distinctly higher than that at the surface. In this case, since MODIS measured the surface temperature, a greater cold difference is inevitable between the MODIS LST and in situ 2 m temperature. When we compared in situ skin temperatures with MODIS LST, high positive correlations demonstrated that inversions still exert a strong influence on the accuracy of MODIS LST, especially on the East Antarctic Plateau, where temperature inversions are more frequent and intense (Connolley, 1996; Scambos and others, 2018). This highly positive correlation suggested that MODIS LST tended to exhibit either warm biases or small cold biases compared to in situ surface temperatures when strong temperature inversions occurred. Some evidence of this can be found in Figure 4 (after removing cloud effects), with some points located far above the 1:1 line, representing the warm biases of MODIS LST in comparison to in situ surface temperatures. Yu and others (1995) showed that ice-crystal precipitation (or clear-sky precipitation) occurring during temperature inversions may cause warm biases of satellite-derived LST compared to ground-based measurements (below the ice-crystal precipitation layer). The East Antarctic Plateau was subjected to frequent temperature inversions and ice-crystal precipitation (Kikuchi and Hogan, 1979; Walden and others, 2003; Vignon and others, 2021), which to some extent explained the occurrence of warm biases and positive correlations between temperature inversions and MODIS LST biases at the Antarctic Plateau stations. Therefore, the influence of atmospheric phenomena occurring simultaneously with inversion and high humidity on MODIS LST accuracy should be examined in the future.

In the coastal region, a 'progressive' cold bias was found that was the bias between two LST datasets gradually increased as the MODIS LST decreased. This was most obvious for the AWS16 station and could also be seen in the scatterplot (Fig. 4e). The MODIS LST exhibited greater cold biases at lower temperatures on the coastal area, indicating that MODIS LST needs to be corrected for low temperatures in the future (Xiong and others, 2015; Zikan and others, 2023).

https://doi.org/10.1017/jog.2024.17 Published online by Cambridge University Press

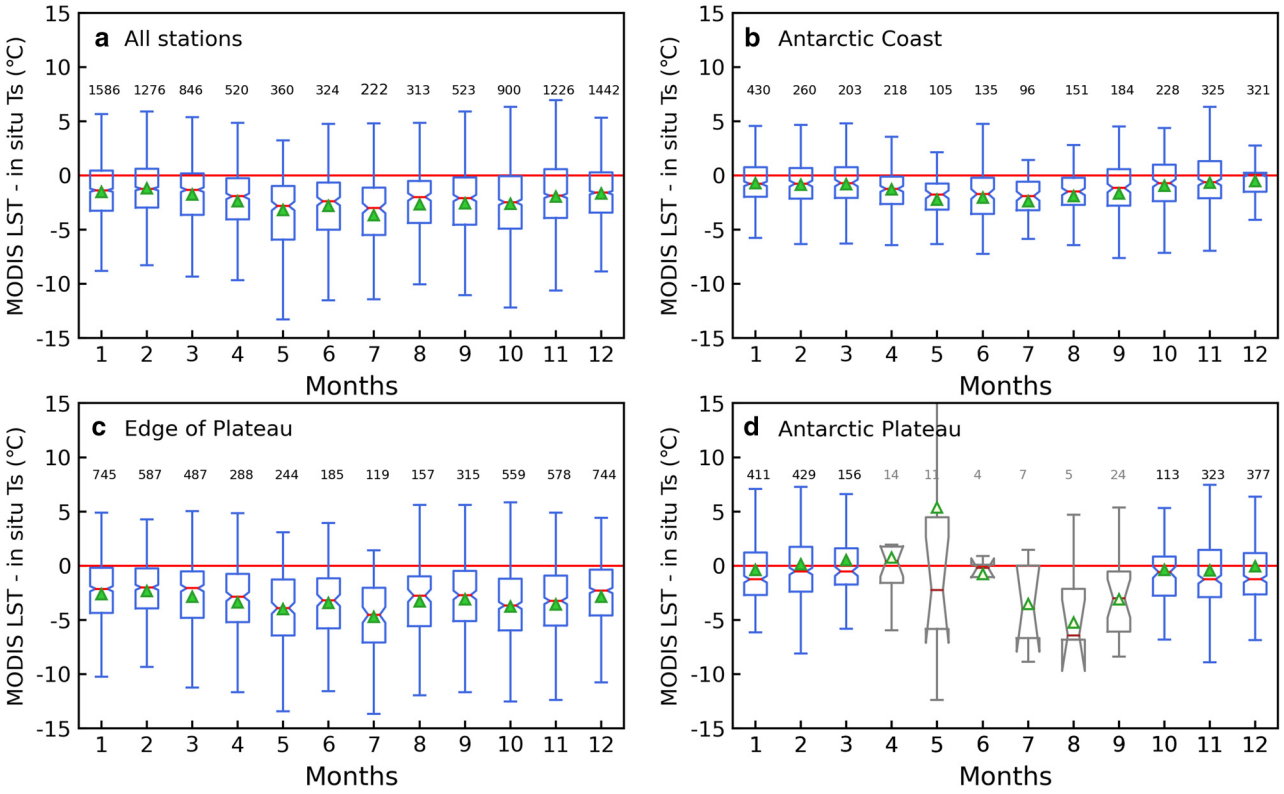

Figure 6. Temperature difference between cloud-screened MODIS LST and in situ T_s in each month at all stations (a), the stations on the Antarctic coast (b), the edge of the plateau (c) and the East Antarctic Plateau (d). Boxplots showed the 25th and 75th percentiles (boxes), the averages (green triangles) and the medians (orange short horizontal lines). The numbers at the top of the boxes were the paired amount of two types of LST observations in each month, and gray boxes in subplot (d) represented the months with fewer than 25 paired amounts. The red horizontal line represented the bias value equal to 0°C. The results cannot be extrapolated to other places without an AWS (equipped with cloud fraction).

We further explored the potential relationships between MODIS LST biases and other environmental factors. Several previous studies reported that biases of C5 and C6 MODIS LST products were associated with the scan angle of the Terra and Aqua satellites (Adolph and others, 2018). However, our study demonstrated that there was no correlation between MODIS LST biases and MODIS view angle in the latest version (C6.1) (Table S1). Furthermore, the latest C6.1 product has undergone improvements in the RVS approach, which affected reflectance bands for Aqua and Terra MODIS (Wan and others, 2021).

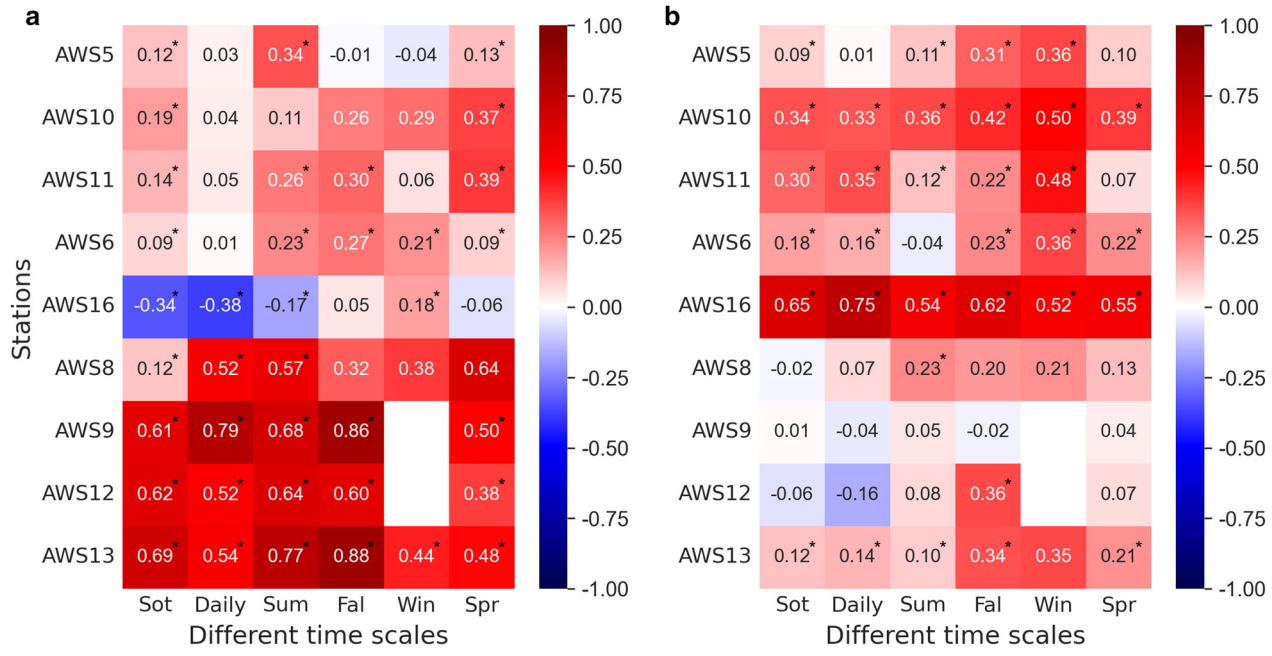

Figure 7. Correlations between biases and (a) near-surface inversions (T_{air}-$T_{surface}$), and (b) MODIS LST at different time scales, respectively. From left to right, the values in each column represented the correlations at satellite overpass time (Sot), daily, austral summer (Sum), fall (Fal), winter (Win) and spring (Spr), respectively. The correlations labeled '*' were significant at $p < 0.05$ level with the two-sided test. The winter at AWS 9 and 12 was filled in white due to the lack of data.

https://doi.org/10.1017/jog.2024.17 Published online by Cambridge University Press

These findings suggested that the impact of the scan angle of satellites have greatly decreased, and likely have been even eliminated. There was no relationship between relative humidity and MODIS LST biases at almost all stations (Table S1), which was inconsistent with the results of Zikan and others (2023) that station-level atmospheric humidity may affect the biases of MODIS LST (C6). Zikan and others (2023) proposed that the presence of hoarfrost growing on sensors under high humidity could cause inaccurate temperature measurements and contribute to errors, but this issue was not found in this study. Additionally, the station-level wind speeds are almost uncorrelated with MODIS LST biases (Table S1). However, a weak negative correlation ($r = -0.22$, $p < 0.05$) was observed between solar radiation and biases at stations on the Antarctic Plateau. We assumed that these relationships were likely linked through temperature inversions, which usually occur at low solar radiation (Table S2 and Fig. S2). Previous results also demonstrated strong and widespread temperature inversions in the interior of Antarctica, but relatively weak in coastal regions (Hudson and Brandt, 2005; Pietroni and others, 2014; Scambos and others, 2018).

Temperature inversions and relative humidity were analyzed on only a narrow vertical scale (at the station level) in this study, and hence it is necessary to explore the temperature inversion intensity and variation of atmospheric water vapor in the thicker atmospheric troposphere, and to investigate its impacts on satellite-derived products in the future. Moreover, the harsh environmental conditions over EAIS such as extreme weather (winds and extremely low temperatures) usually result in intermittent gaps in AWS meteorological observations (Zhang and others, 2022). This somewhat limited our study of factors affecting MODIS LST accuracy, especially in winter (Fig. 7).

5. Conclusions

MODIS has proved to be a valuable tool for monitoring surface temperatures across East Antarctica. The latest MODIS LST C6.1 product highly and significantly correlated with in situ T_s calculated by radiation from 12 stations in East Antarctica, with the determination coefficient (R^2) of >0.75 at most stations. However, there was no distinct improvement in the C6.1 MODIS LST over C5 version on the EAIS. Significant cold biases occurred in MODIS LST at different timescales (transient, daily and monthly), and these biases were more pronounced during cold period than during warm period. Spatially, the biases were smaller at inland stations, but larger for the stations on coastal regions and the edge of plateau. The cloud fraction, low temperature and near-surface temperature inversion intensity contributed much to the MODIS LST biases. Cloud contamination was effectively removed by utilizing a stricter filter based on AWS cloud fraction, which thereby significantly improved MODIS LST accuracy. Therefore, there was a need to develop a more stringent cloud mask algorithm to further reduce cloud effects on MODIS LST product, especially at the Antarctic coastal regions. The application of AWS observations was a good choice for improving MODIS cloud mask algorithm. Low temperature corrections were also required in coastal regions. In addition, on the Antarctic Plateau, ice-crystal precipitation occurring during temperature inversions significantly impacted the MODIS LST biases. The energy balance model appears to be a promising approach for calibrating MODIS LST in the future research. Notably, validating satellite-generated LST observations in East Antarctica remains challenging due to the sparseness of in situ observations. Therefore, strengthening in situ LST monitoring particularly during winter is highly needed.

Supplementary material. The supplementary material for this article can be found at https://doi.org/10.1017/jog.2024.17.

Data. The MODIS LST products used in this study are available at http://modis.gsfc.nasa.gov. The AWSs datasets are available at https://doi.org/10.1594/PANGAEA.910473 and the BSRN stations datasets are available at https://dataportals.pangaea.de/bsrn/3. The unpublished data used in this paper can be obtained by contacting the author if they are needed.

Acknowledgements. This work was financially supported by the National Key Research and Development Program of China (2020YFA0608202), the National Natural Science Foundation of China (41971081 and 41830644), the Strategic Priority Research Program of the Chinese Academy of Sciences (XDA19070103) and the Project for Outstanding Youth Innovation Team in the Universities of Shandong Province (2019KJH011). The authors are grateful for the comments from Ghislain Picard (reviewer) and the anonymous reviewer which have improved this manuscript.

Competing interest. None.

References

Adolph AC, Albert MR and Hall DK (2018) Near-surface temperature inversion during summer at Summit, Greenland, and its relation to MODIS-derived surface temperatures. *The Cryosphere* **12**(3), 907–920. doi: 10.5194/tc-12-907-2018

Allison L, Wendler G and Radok U (1993) Climatology of the East Antarctic ice sheet (100°E to 140°E) derived from automatic weather stations. *Journal of Geophysical Research: Atmospheres* **98**(D5), 8815–8823. doi: 10.1029/93JD00104

Amesbury MJ and 6 others (2017) Widespread biological response to rapid warming on the Antarctic Peninsula. *Current Biology* **27** (11), 1616–1622. doi: 10.1016/j.cub.2017.04.034

Ayanlade A (2016) Variation in diurnal and seasonal urban land surface temperature: land use change impacts assessment over Lagos metropolitan city. *Modeling Earth Systems and Environment* **2**, 1–8. doi: 10.1007/s40808-016-0238-z

Baumhoer CA, Dietz AJ, Kneisel C, Paeth H and Kuenzer C (2021) Environmental drivers of circum-Antarctic glacier and ice shelf front retreat over the last two decades. *The Cryosphere* **15**(5), 2357–2381. doi: 10.5194/tc-15-2357-2021

Bromwich DH and Wang SH (2008) A review of the temporal and spatial variability of Arctic and Antarctic atmospheric circulation based upon ERA-40. *Dynamics of Atmospheres and Oceans* **44**(3), 213–243. doi: 10.1016/j.dynatmoce.2007.09.001

Brun E and 12 others (2011) Snow/atmosphere coupled simulation at Dome C, Antarctica. *Journal of Glaciology* **57** (204), 721–736. doi: 10.3189/002214311797409794

Clem KR and Fogt RL (2015) South Pacific circulation changes and their connection to the tropics and regional Antarctic warming in austral spring, 1979-2012. *Journal of Geophysical Research: Atmospheres* **120**(7), 2773–2792. doi: 10.1002/2014JD022940

Coll C and 6 others (2005) Ground measurements for the validation of land surface temperatures derived from AATSR and MODIS data. *Remote Sensing of Environment* **97** (3), 288–300. doi: 10.1016/j.rse.2005.05.007

Coll C, Wan Z and Galvem JM (2009) Temperature-based and radiance-based validations of the V5 MODIS land surface temperature product. *Journal of Geophysical Research* **114**(D20), D20102. doi: 10.1029/2009JD012038

Comiso JC (2000) Variability and trends in Antarctic surface temperatures from in situ and satellite infrared measurements. *Journal of Climate* **13**, 1674–1696. doi: 10.1175/1520-0442(2000)013<1674:VATIAS>2.0.CO;2

Connolley WM (1996) The Antarctic temperature inversion. *International Journal of Climatology* **16**(12), 1333–1342. doi: 10.1002/(SICI)1097-0088(199612)16:12<1333::AID-JOC96>3.0.CO;2-6

Crosman EA and Horel JD (2009) MODIS-derived surface temperature of the Great Salt Lake. *Remote Sensing of Environment* **113**(1), 73–81. doi: 10.1016/j.rse.2008.08.013

DeConto R and Pollard D (2016) Contribution of Antarctica to past and future sea-level rise. *Nature* **531**, 591–597. doi: 10.1038/nature17145

Dozier J and Warren S (1982) Effect of viewing angle on the infrared brightness temperature of snow. *Water Resources Research* **18**(5), 1424–1434. doi: 10.1029/WR018i005p01424

Driemel A and 37 others (2018) Baseline Surface Radiation Network (BSRN), structure and data description (1992–2017). *Earth System Science Data* **10**, 1491–1501. doi: 10.5194/essd-10-1491-2018

Duan SB and 5 others (2018) Radiance-based validation of land surface temperature products derived from Collection 6 MODIS thermal infrared data. *International Journal of Applied Earth Observation and Geoinformation* **70**, 84–92. doi: 10.1016/j.jag.2018.04.006

Duan SB, Li ZL, Cheng J and Leng P (2017) Cross-satellite comparison of operational land surface temperature products derived from MODIS and ASTER data over bare soil surfaces. *ISPRS Journal of Photogrammetry and Remote Sensing* **126**, 1–10. doi: 10.1016/j.isprsjprs.2017.02.003

Freville H and 7 others (2014) Using MODIS land surface temperatures and the Crocus snow model to understand the warm bias of ERA-Interim reanalyses at the surface in Antarctica. *The Cryosphere* **8** (4), 1361–1373. doi: 10.5194/tc-8-1361-2014

Graversen R, Mauritsen T, Tjernström M, Källén E and Svensson G (2008) Vertical structure of recent Arctic warming. *Nature* **451**, 53–56. doi: 10.1038/nature06502

Hall DK and 5 others (2008) Comparison of satellite-derived and in-situ observations of ice and snow surface temperatures over Greenland. *Remote Sensing of Environment* **112** (10), 3739–3749. doi: 10.1016/j.rse.2008.05.007

Hall DK and 5 others (2013) Variability in the surface temperature and melt extent of the Greenland ice sheet from MODIS. *Geophysical Research Letters* **40** (10), 2114–2120. doi: 10.1002/grl.50240

Hall DK, Key JR, Casey KA, Riggs GA and Cavalieri DJ (2004) Sea ice surface temperature product from MODIS. *IEEE Transactions on Geoscience and Remote Sensing* **42**(5), 1076–1087. doi: 10.1109/TGRS.2004.825587

Hudson SR and Brandt RE (2005) A look at the surface-based temperature inversion on the Antarctic plateau. *Journal of Climate* **18**(11), 1673–1696. doi: 10.1175/JCLI3360.1

Jacob F and 5 others (2004) Comparison of land surface emissivity and radiometric temperature derived from MODIS and ASTER sensors. *Remote Sensing of Environment* **90** (2), 137–152. doi: 10.1016/j.rse.2003.11.015

Jakobs CL, Carleen HR, Michiel R, Smeets CJPP and Gert KL (2020) High-resolution meteorological observations, surface energy balance components and miscellaneous data from 10 AWS and one staffed station in Antarctica [Data set]. *PANGAEA*. doi: 10.1594/PANGAEA.910473

Justice CO and 22 others (1998) The Moderate Resolution Imaging Spectroradiometer (MODIS): land remote sensing for global change research. *IEEE Transactions on Geoscience and Remote Sensing* **36**(4), 1228–1249. doi: 10.1109/36.701075

Kang D, Im J, Lee MI and Quackenbush LJ (2014) The MODIS ice surface temperature product as an indicator of sea ice minimum over the Arctic Ocean. *Remote Sensing of Environment* **152**, 99–108. doi: 10.1016/j.rse.2014.05.012

Kikuchi K and Hogan AW (1979) Properties of diamond dust type ice crystals observed in summer season at Amundsen-Scott south pole station, Antarctica. *Journal of the Meteorological Society of Japan. Ser. II* **57**(2), 180–190. doi: 10.2151/jmsj1965.57.2_180

Kilpatrick KA and 8 others (2015) A decade of sea surface temperature from MODIS. *Remote Sensing of Environment* **165**, 27–41. doi: 10.1016/j.rse.2015.04.023

Kindstedt I and 6 others (2022) Offset of MODIS land surface temperatures from in situ air temperatures in the upper Kaskawulsh Glacier region (St. Elias Mountains) indicates near-surface temperature inversions. *The Cryosphere* **16** (8), 3051–3070. doi: 10.5194/tc-16-3051-2022

Koenig LS and Hall DK (2010) Comparison of satellite, thermochron and air temperatures at Summit, Greenland, during the winter of 2008/09. *Journal of Glaciology* **56**(198), 735–741. doi: 10.3189/002214310793146269

Kuipers Munneke P, Reijmer CH and van den Broeke MR (2011) Assessing the retrieval of cloud properties from radiation measurements over snow and ice. *International Journal of Climatology* **31**(5), 756–769. doi: 10.1002/joc.2114

Kumari B and 6 others (2018) Satellite-driven land surface temperature (LST) using Landsat 5, 7 (TM/ETM + SLC) and Landsat 8 (OLI/TIRS) data and its association with built-up and green cover over Urban Delhi, India. *Remote Sensing in Earth Systems Sciences* **1**, 63–78. doi: 10.1007/s41976-018-0004-2

Lazzara M, Weidner G, Keller L, Thom J and Cassano J (2012) Antarctic automatic weather station program: 30 years of polar observation. *Bulletin of the American Meteorological Society* **93**(10), 1519–1537. doi: 10.1175/BAMS-D-11-00015.1

Li H and 8 others (2014) Evaluation of the VIIRS and MODIS LST products in an arid area of Northwest China. *Remote Sensing of Environment* **142**, 111–121. doi: 10.1016/j.rse.2013.11.014

Liu T and 5 others (2015) An effective Antarctic ice surface temperature retrieval method for MODIS. *Photogrammetric Engineering & Remote Sensing* **81** (11), 861–872. doi: 10.14358/PERS.81.11.861

Mengel M and Levermann A (2014) Ice plug prevents irreversible discharge from East Antarctica. *Nature Climate Change* **4**, 451–455. doi: 10.1038/nclimate2226

Miles B, Stokes C and Vieli A (2013) Rapid, climate-driven changes in outlet glaciers on the Pacific coast of East Antarctica. *Nature* **500**, 563–566. doi: 10.1038/nature12382

Muster S, Langer M, Abnizova A, Young KL and Boike J (2015) Spatio-temporal sensitivity of MODIS land surface temperature anomalies indicate high potential for large-scale land cover change detection in Arctic permafrost landscapes. *Remote Sensing of Environment* **168**, 1–12. doi: 10.1016/j.rse.2015.06.017

Nghiem SV and 8 others (2012) The extreme melt across the Greenland ice sheet in 2012. *Geophysical Research Letters* **39** (20), L20502. doi: 10.1029/2012GL053611

Nguemhe Fils SC and 5 others (2018) TM/ETM + /LDCM images for studying land surface temperature (LST) interplay with impervious surfaces changes over time within the Douala Metropolis, Cameroon. *Journal of the Indian Society of Remote Sensing* **46**, 131–143. doi: 10.1007/s12524-017-0677-7

Østby TI, Schuler TV and Westermann S (2014) Severe cloud contamination of MODIS land surface temperatures over an Arctic ice cap, Svalbard. *Remote Sensing of Environment* **142**, 95–102. doi: 10.1016/j.rse.2013.11.005

Pattyn F and Morlighem M (2020) The uncertain future of the Antarctic ice sheet. *Science* **367**(6484), 1331–1335. doi: 10.1126/science.aaz5487

Pietroni I, Argentini S and Petenko I (2014) One year of surface-based temperature inversions at Dome C, Antarctica. *Boundary-Layer Meteorology* **150**, 131–151. doi: 10.1007/s10546-013-9861-7

Qie Y, Wang N, Wu Y and Chen A (2020) Variations in winter surface temperature of the Purog Kangri Ice Field, Qinghai–Tibetan Plateau, 2001–2018, using MODIS data. *Remote Sensing* **12**(7), 1133. doi: 10.3390/rs12071133

Remy F and Frezzotti M (2006) Antarctica ice sheet mass balance. *Comptes Rendus Geoscience* **338**(14-15), 1084–1097. doi: 10.1016/j.crte.2006.05.009

Retamales MG, Durán-Alarcón C and Mattar C (2019) Recent land surface temperature patterns in Antarctica using satellite and reanalysis data. *Journal of South American Earth Sciences* **95**, 02304. doi: 10.1016/j.jsames.2019.102304

Rignot E and 6 others (2008) Recent Antarctic ice mass loss from radar interferometry and regional climate modelling. *Nature Geoscience* **1**, 106–110. doi: 10.1038/ngeo102

Scambos TA and 7 others (2018) Ultralow surface temperatures in East Antarctica from satellite thermal infrared mapping: the coldest places on earth. *Geophysical Research Letters* **45** (12), 6124–6133. doi: 10.1029/2018GL078133

Scambos TA, Haran TM and Massom R (2006) Validation of AVHRR and MODIS ice surface temperature products using in situ radiometers. *Annals of Glaciology* **44**, 345–351. doi: 10.3189/172756406781811457

Screen JA, Bracegirdle TJ and Simmonds I (2018) Polar climate change as manifest in atmospheric circulation. *Current Climate Change Reports* **4**, 383–395. doi: 10.1007/s40641-018-0111-4

Seo M and 7 others (2016) Long-term variability of surface albedo and its correlation with climatic variables over Antarctica. *Remote Sensing* **8**(12), 981. doi: 10.3390/rs8120981

Steig E and 5 others (2009) Warming of the Antarctic ice-sheet surface since the 1957 International Geophysical Year. *Nature* **457**, 459–462. doi: 10.1038/nature07669

Studinger M and 5 others (2005) Science opportunities for a long-range Antarctic research aircraft. *Eos, Transactions, American Geophysical Union* **86**(4), 39–40. doi: 10.1029/2005EO040004

Sun L and 7 others (2017) Reconstructing daily clear-sky land surface temperature for cloudy regions from MODIS data. *Computers & Geosciences* **105**, 10–20. doi: 10.1016/j.cageo.2017.04.007

Tan K, Liao Z, Du P and Wu L (2017) Land surface temperature retrieval from Landsat 8 data and validation with geosensor network. *Frontiers of Earth Science* **11**, 20–34. doi: 10.1007/s11707-016-0570-7

Tuckett PA and 6 others (2019) Rapid accelerations of Antarctic Peninsula outlet glaciers driven by surface melt. *Nature Communications* **10**, 4311. doi: 10.1038/s41467-019-12039-2

Turner J and 8 others (2004) The SCAR READER Project: toward a high-quality database of mean Antarctic meteorological observations. *Journal of Climate* **17** (14), 2890–2898. doi: 10.1175/1520-0442(2004)017<2890:TSRPTA>2.0.CO;2

https://doi.org/10.1017/jog.2024.17 Published online by Cambridge University Press

Vaughan DG and 8 others (2003) Recent rapid regional climate warming on the Antarctic Peninsula. *Climatic Change* **60**, 243–274. doi: 10.1023/A:1026021217991

Vignon É, Roussel ML, Gorodetskaya IV, Genthon C and Berne A (2021) Present and future of rainfall in Antarctica. *Geophysical Research Letters* **48**(8), e2020GL092281. doi: 10.1029/2020GL092281

Walden W, Warren SG and Tuttle E (2003) Atmospheric ice crystals over the Antarctic Plateau in winter. *Journal of Applied Meteorology and Climatology* **42**(10), 1391–1405. doi: 10.1175/1520-0450(2003)042<1391:AICOTA>2.0.CO;2

Wan Z (2008) New refinements and validation of the MODIS land-surface temperature/emissivity products. *Remote Sensing of Environment* **112**(1), 59–74. doi: 10.1016/j.rse.2006.06.026

Wan Z (2014) New refinements and validation of the collection-6 MODIS land surface temperature/emissivity product. *Remote Sensing of Environment* **140**, 36–45. doi: 10.1016/j.rse.2013.08.027

Wan Z and Dozier J (1996) A generalized split-window algorithm for retrieving land-surface temperature from space. *IEEE Transactions on Geoscience and Remote Sensing* **34**(4), 892–905. doi: 10.1109/36.508406

Wan Z, Hook S and Hulley G (2021) MODIS/Aqua Land Surface Temperature/Emissivity 5-Min L2 Swath 1 km V061. distributed by NASA EOSDIS Land Processes Distributed Active Archive Center. doi: 10.5067/MODIS/MYD11_L2.061

Wan Z, Zhang Y, Zhang Q and Li ZL (2002) Validation of the land-surface temperature products retrieved from Terra Moderate Resolution Imaging Spectroradiometer data. *Remote Sensing of Environment* **83**(1–2), 163–180. doi: 10.1016/S0034-4257(02)00093-7

Wan Z, Zhang Y, Zhang Q and Li ZL (2004) Quality assessment and validation of the MODIS global land surface temperature. *International Journal of Remote Sensing* **25**(1), 261–274. doi: 10.1080/0143116031000116417

Wang Y and 15 others (2023) The AntAWS dataset: a compilation of Antarctic automatic weather station observations. *Earth System Science Data* **15**(1), 411–429. doi: 10.5194/essd-15-411-2023

Wang K and Liang S (2009) Evaluation of ASTER and MODIS land surface temperature and emissivity products using long-term surface longwave radiation observations at SURFRAD sites. *Remote Sensing of Environment* **113**(7), 1556–1565. doi: 10.1016/j.rse.2009.03.009

Wang Y, Wang M and Zhao J (2013) A comparison of MODIS LST retrievals with in situ observations from AWS over the Lambert Glacier Basin, East Antarctica. *International Journal of Geosciences* **4**(3), 611–617. doi: 10.4236/ijg.2013.43056

Westermann S, Langera M and Boikea J (2012) Systematic bias of average winter-time land surface temperatures inferred from MODIS at a site on Svalbard, Norway. *Remote Sensing of Environment* **118**, 162–167. doi: 10.1016/j.rse.2011.10.025

Williamson SN and 6 others (2017) Spring and summer monthly MODIS LST is inherently biased compared to air temperature in snow covered sub-Arctic mountains. *Remote Sensing of Environment* **189**, 14–24. doi:10.1016/j.rse.2016.11.009

Wong TE, Bakker AMR and Keller K (2017) Impacts of Antarctic fast dynamics on sea-level projections and coastal flood defense. *Climatic Change* **144**, 347–364. doi: 10.1007/s10584-017-2039-4

Xiong X and 8 others (2015) Terra and Aqua MODIS thermal emissive bands on-orbit calibration and performance. *IEEE Transactions on Geoscience and Remote Sensing* **53** (10), 5709–5721. doi: 10.1109/TGRS.2015.2428198

Xu Y and Shen Y (2013) Reconstruction of the land surface temperature time series using harmonic analysis. *Computers & Geosciences* **61**, 126–132. doi: 10.1016/j.cageo.2013.08.009

Yu Y, Rothrock DA and Lindsay RW (1995) Accuracy of sea ice temperature derived from the advanced very high resolution radiometer. *Journal of Geophysical Research: Oceans* **100**(C3), 4525–4532. doi: 10.1029/94JC02244

Zhang X and 6 others (2022) Spatiotemporal reconstruction of Antarctic near-surface air temperature from MODIS observations. *Journal of Climate* **35** (17), 5537–5553. doi: 10.1175/JCLI-D-21-0786.1

Zhang X, Tan SC and Shi GY (2018) Comparison between MODIS-derived day and night cloud cover and surface observations over the North China Plain. *Advances in Atmospheric Sciences* **35**, 146–157. doi: 10.1007/s00376-017-7070-x

Zikan K, Adolph A, Brown W and Fausto R (2023) Comparison of MODIS surface temperatures to in situ measurements on the Greenland ice sheet from 2014 to 2017. *Journal of Glaciology* **69**(273), 129–140. doi: 10.1017/jog.2022.51

https://doi.org/10.1017/jog.2024.17 Published online by Cambridge University Press